

Different strategies for cancer treatment: mathematical modeling

O.G. Isaeva^{1,*}, and V.A. Osipov¹

¹ *Bogoliubov Laboratory of Theoretical Physics, Joint Institute for Nuclear Research, 141980, Dubna, Moscow region, Russia*

Abstract

We formulate and analyze a mathematical model describing tumor-immune dynamics under the influence of immunotherapy and chemotherapy and their combinations as well as vaccine treatments. For low-immunogenic tumor, neither immunotherapy nor chemotherapy is found to cause tumor regression to a small size, which would be below the clinically detectable threshold. The effect of vaccine therapy is considered as a parametric perturbation of the model. Numerical simulations show that the efficiency of vaccine therapy depends on both the tumor size and the condition of immune system as well as on the response of the organism to vaccination. In particular, we found that vaccine therapy becomes more effective when used without time delay from a prescribed date of vaccination after surgery and is ineffective without preliminary treatment. Our study of successive chemo/immuno, immuno/chemo and concurrent immuno/chemo therapy shows that the chemo/immunotherapy sequence is more effective while concurrent chemo/immunotherapy is more sparing.

Key words: anti-tumor immune response, mathematical modeling, chemotherapy, immunotherapy, vaccine, cancer

* Corresponding author. Current addresses: Bogoliubov Laboratory of Theoretical Physics, Joint Institute for Nuclear Research, 141980, Dubna, Moscow region, Russia. Fax.: (7)(49621)65084. E-mail addresses: issaeva@theor.jinr.ru, osipov@theor.jinr.ru.

1. Introduction

According to statistics, the oncological mortality takes second place just after cardiovascular diseases. Indeed, treatment of cancer is very difficult because tumor cell division process is unlimited. Besides, tumor cells are able to invade into neighboring tissues and give metastases. Unfortunately, for chemo and radiotherapy, which seemed to have potential to eliminate tumor cells, a number of healthy cells (including immune cells) turn out to be also damaged. Hence, a simple increase of the impact dose does not solve the problem of cancer treatment because this leads to the damage of normal tissues as well as to the suppression of immune functions. Modern treatment methods include improved traditional surgery, chemotherapy and radiotherapy as well as immunotherapy. As is well known, tumors stimulate immune response [2,27]. The fact that the immune system plays an important role in fighting cancer has been verified both in laboratorial and clinical experiments [13,25]. An inclusion of immune component in mathematical models of tumor growth has been shown to reflect clinically observed phenomena such as tumor dormancy and oscillations in tumor size [1,8,14,21,31,34]. A similar tumor behavior was also predicted in our recent model [20] with the interleukine-2 (IL-2) taken into account.

One of the modern trends in treatment of cancer is immunotherapy. The goal of immunotherapy is to enhance the anti-tumor resistance of an organism and improve the immune system condition. There are known three main categories of immunotherapy: immune response modifiers (cytokines), monoclonal antibodies and vaccines [28]. Such immune modifiers as IL-2, interferon- α (IFN- α) as well as tumor necrosis factor- α (TNF- α) are already widely used in cancer immunotherapy [4,5,17,18,29,35]. An important problem is to choose the correct schedule for using chemotherapy in combination with IL-2 and IFN- α therapy. In particular, the clinical trials show that cisplatin-based treatment of metastatic melanoma in combination with IFN- α and IL-2 is most favorable [4,5]. This finding stimulated our interest to consider within our model the effects of sequential chemo-immuno therapy. Monoclonal antibodies (MA) are used in both diagnostics and therapy of cancer. This follows from ability of MA to recognize tumor antigens on a surface of tumor cells. As a result, MA can deliver both anti-tumor drugs and radioactive isotopes exactly to the malignant cells [22,26]. Notice that cancer vaccines are still under experimental investigations. Nevertheless, the existent clinical trials clearly show that the cancer vaccine can improve immune response to certain forms of cancer [28,36]. Notice that most of cancer vaccines consist of living tumor cells and their lysis products while some of them contain tumor-derived proteins, peptides and gangliosides [30]. For instance, an experimental vaccine for malignant melanoma consists of four melanoma peptides and includes also IL-2 and granulocyte macrophage colony stimulating factor (GM-CSF). It was found that this vaccination is able to stimulate tumor regression in some cases [32,33].

One of the first attempts to consider effects of immunotherapy within an appropriate mathematical model was made by Kirschner and Panetta (1998) in [21]. They study immunotherapy based on the use of IL-2 together with adoptive cellular immunotherapy (ACI) by introducing in dynamical equations terms describing external inflow of both IL-2 and cultured immune cells. It should be noted that these terms are considered to be time independent. More recently, de Pillis et al., (2003) have proposed the model of anti-tumor immune response

where individual equations were suggested for the description of mechanisms of natural immunological defense presented by NK-cells and specific immune response presented by CD8+ T cells [10,11]. Notice, that unlike Kirschner and Panetta, (1998) [21] they do not consider a natural dynamics of IL-2. In the framework of this model the effects of chemotherapy, immunotherapy, their combined influence, as well as the vaccine therapy were considered [11]. It was shown that immunotherapy gives best results in combination with chemotherapy. Similarly, the vaccine therapy is found to be more effective in combination with chemotherapy. At the same time, dramatic tumor regression was observed that is sensitive to the choice of tumor and patient parameters, as well as to the timing of treatments [11].

Finally, it is interesting to mention a recent paper by Arciero et al. (2004) [3] where a novel treatment strategy known as small interfering RNA (siRNA) therapy is considered in the framework of the model proposed in [21]. Notice that siRNA treatment suppresses TGF- β production by targeting the mRNA codes for TGF- β , thereby reducing the presence and effect of TGF- β in tumor cells. The model predicts conditions under which siRNA treatment can be successful in transformation of TGF- β producing tumors to either non-producing or producing a small value of TGF- β tumors, that is to a non-immune evading state.

The outline of the present paper is as follows. First of all, based on our previous work [20], a mathematical model of tumor-immune dynamics under the influence of both immunotherapy with IL-2 and IFN- α and chemotherapy is formulated in section 2. In section 3 we perform a steady state analysis of the model. The results of numerical studies are presented in section 4 for four different cases: chemotherapy alone, IL-2 alone, IL-2 plus IFN- α , and a combination of chemotherapy and immunotherapy (IL-2 therapy). The effects of vaccine therapy are considered in the absence of chemotherapy and immunotherapy in section 4. Section 5 is devoted to conclusions and discussion.

2. Mathematical model

As already noted, clinical trials of mixed chemoimmunotherapy are developed for metastatic melanoma treatment. In particular, a series of sequential phase II trials were conducted at M. D. Anderson Cancer Center (MDACC) (see, e.g., [4,5]). These trials were based on integrating of IL-2 and IFN- α with the CVD (cisplatin, vinblastine, and dacarbazine) regimen. It was found that chemotherapy followed immediately by immunotherapy (IL-2 and IFN- α) is more effective than their reverse sequence. Concurrent chemoimmunotherapy is almost as effective as chemo/immune sequence when immunotherapy is administered right after the CVD. Notice, however, that the concurrent biochemotherapy is found to be less toxic than the sequential regimens [5].

In order to study the effects of mixed chemoimmunotherapy within a mathematical model one has to introduce terms describing chemotherapy and immunotherapy effects as well as additional equations for therapeutic drug and IFN- α . To this end, we will extend our model proposed in [20] for the description of the tumor-immune dynamics with IL-2 taken into account. The modified model reads

$$\dot{\xi} = -a_{\xi} \xi \ln \frac{b_{\xi} \xi}{a_{\xi}} - c_{\xi} (\alpha) \xi \eta - d_{\xi} (\zeta) (1 - e^{-\phi}) \xi, \quad (1)$$

$$\dot{\eta} = V_{\eta} + a_{\eta} \eta \zeta - b_{\eta} \eta - d_{\eta}(\zeta)(1 - e^{-\phi}) \eta, \quad (2)$$

$$\dot{\zeta} = V_{\zeta}(t) + \frac{a_{\zeta} \xi}{\xi + K_{\xi}} - \tilde{a}_{\eta} \eta \zeta - c_{\zeta} \xi \zeta, \quad (3)$$

$$\dot{\phi} = V_{\phi}(t) - b_{\phi} \phi, \quad (4)$$

$$\dot{\alpha} = V_{\alpha}(t) - b_{\alpha} \alpha, \quad (5)$$

The system (1)—(5) describes the most important components of tumor-immune dynamics in the presence of treatment components. Namely, we consider five populations: tumor cells (ξ), cytotoxic T lymphocytes — CTL (η), IL-2 (ζ), chemotherapeutic drug (ϕ), and IFN- α (α). We choose the Gompertzian law for tumor growth in the absence of the immune activity (the first term in (1)). The destruction of tumor cells by CTL is presented by the second term in (1). It is supposed that the destruction rate is proportional to the number of tumor cells and CTL populations. In (2) V_{η} characterizes the steady inflow of CTL from stem cells. The second term in (2) describes CTL proliferation in response to the IL-2 action. The third term describes CTL death rate. In (3)—(5) V_i ($i=\zeta, \phi, \alpha$) describes the external influxes of IL-2, chemotherapeutic drug and IFN- α , respectively. Since therapy is assigned to a certain schedule, these influxes are taken to be time-dependent. IL-2 production in (3) is described by hyperbola (the second term), which allows us to take into account a limitation in the stimulation of the immune system by the growing tumor. At small ξ the growth rate is nearly linear in tumor size while for big tumor ($\xi \gg K_{\xi}$) it tends to a maximum constant value a_{ζ} . The parameter K_{ξ} influences the IL-2 production rate. The smaller is the value of K_{ξ} , the quicker the IL-2 production rate achieves its maximum value a_{ζ} . Notice that a_{ζ} characterizes the degree of expression of the antigen plus major histocompatibility complexes class II (AG-MHC-II) on the APC surfaces, i.e. the antigen presentation. The probability of activation (provoking the IL-2 production) of helper T cell precursor by the APC increases with the antigen presentation. Since IL-2 is a short-distance cytokine, it is suggested that target cells (cytotoxic T lymphocytes) effectively consume IL-2. The consumption rate is presented by the term $\tilde{a}_{\eta} \eta \zeta$ in (3). It was found that inhibition of IL-2 results from an accumulation of immune-suppressing substances, prostaglandins. Their number is proportional to the concentration of tumor cells. Prostaglandins suppress the production of IL-2 and can directly destroy its molecules [23]. In (3) the IL-2 destruction rate is described by $c_{\zeta} \xi \zeta$.

Some chemotherapeutic drugs, for instance dacarbazine, become more effective only during certain phases of cell cycle. Their pharmacokinetic features also indicate that the effectiveness of chemotherapy is limited. Therefore, similarly to [11], we use in Eqs. (1) and (2) a saturation term $d_j(\zeta)(1 - e^{-\phi})j$ with $j = \xi, \eta$ to describe cell death caused by chemotherapeutic drug. Notice that at low concentrations the death rate is nearly linear in drug while at higher concentrations the death rate turns out to be ϕ -independent. As was noted in [11] this behavior shows a good correlation with existing dose-response curves (see, e.g., [16]).

According to present views, the enhancement of the chemotherapeutic effect by immunotherapy takes place due to the fact that IL-2 can induce the second cytokines, for instance TNF- α [4]. These cytokines can either promote DNA damages or inhibit DNA repair. In order to take proper account of this possibility we assume that d_j depends on the IL-2 concentration in the following way: $d_j(\zeta) = d_j^{\text{chemo}} (2 - e^{-\zeta/\zeta_0})$. Thus, d_j increases with the concentration of IL-2, however, it never exceeds a doubled value of d_j^{chemo} (cell killing by chemotherapy).

IFN- α is a cytokine produced by the immune cells of the most of animals in response to alien agents such as viruses, bacteria, parasites and tumor cells. The experimental data show that IFN- α directly inhibits the growth of some tumor cell lines *in vitro* [35]. IFN- α also enhances immune-mediated anti-tumor responses by increasing the NK cell activity and modulating survival of CTL as well as by increasing expression of MHC molecules on tumor cells, thus enhancing their recognition by CTL [35]. Therefore, we suppose that the model parameter c_ξ in (1) depends on the IFN- α concentration as $c_\xi(\alpha) = c_\xi^{\text{CTL}} (2 - e^{-\alpha/\alpha_0})$, where c_ξ^{CTL} is a rate of tumor cells inactivation by CTL. Notice that only therapeutic IFN- α dynamics is considered within our model. Finally, the system of equations takes the following form:

$$\dot{\xi} = -a_\xi \xi \ln \frac{b_\xi \xi}{a_\xi} - c_\xi^{\text{CTL}} (2 - e^{-\alpha/\alpha_0}) \xi \eta - d_\xi^{\text{chemo}} (2 - e^{-\zeta/\zeta_0}) (1 - e^{-\phi}) \xi, \quad (6)$$

$$\dot{\eta} = V_\eta + a_\eta \eta \zeta - b_\eta \eta - d_\eta^{\text{chemo}} (2 - e^{-\zeta/\zeta_0}) (1 - e^{-\phi}) \eta, \quad (7)$$

$$\dot{\zeta} = V_\zeta(t) + \frac{a_\zeta \xi}{\xi + K_\xi} - \tilde{a}_\eta \eta \zeta - c_\zeta \xi \zeta, \quad (8)$$

$$\dot{\phi} = V_\phi(t) - b_\phi \phi, \quad (9)$$

$$\dot{\alpha} = V_\alpha(t) - b_\alpha \alpha, \quad (10)$$

For simplicity we do not consider here such processes as angiogenesis (vascular growth), invasion and metastasis, which are of importance at late (III-IV) stages of the tumor growth. Notice that inclusion of processes of vascular growth and invasion requires serious extension of the model to describe dynamics of cytokines, enzymes and other components regulating these processes. Besides, it would be necessary to take into account spatial migration of cell populations during the process of invasion (see, e.g., [7]). Finally, individual character of metastases calls for a specific for each metastasis model. Therefore, the system (6)—(10) is valid for the description of early stages of the tumor growth when the processes of angiogenesis, invasion and metastasis are not of critical importance.

2.1. Estimation of parameters

Evidently, possible scenarios of tumor-immune dynamics are very sensitive to the choice of the parameters in the model equations (6)—(10). In fact the

parameter sets vary not only for specific cancer types but also from one individual to another. The model study is based on using of some generalized (most typical) parameters. In order to reflect individual clinical response to emerging treatment, in this paper we utilize two parameter sets shown in Table 1. Some values of these parameters were estimated by using the available experimental data. In particular, the human melanoma growth parameters in the absence of the immune response were estimated by means of the least-squares method using the data from [19]. The parameters characterizing the cell death caused by chemotherapeutic influence were taken from [11]. The elimination rates for chemotherapeutic drug (dacarbazine) and IFN- α were calculated using their well-known half-life times and the relation $b_i = \ln 2/t_{i/2}$ where $i = \varphi, \alpha$ (see [24,37]).

2.2. Scaling

For convenience, similarly to [20], let us introduce dimensionless variables and parameters as follows: $\xi' = \xi/\xi_0$, $\eta' = \eta/\eta_0$, $\zeta' = \zeta/\zeta_0$, $\alpha' = \alpha/\alpha_0$ and $t' = t/\tau$, where $\tau = b_\eta^{-1}$ (days). The values of ξ_0 , η_0 , ζ_0 and α_0 are given in accordance with [15,21] and presented in Table 1. Notice that the variable for chemotherapeutic drug, φ , is given in relative units. The choice of the time-scale factor τ is based on the fact that the mean lifetime of CTL is about three days and a similar time is needed for the proliferation of CTL and IL-2 production [6,9].

In dimensionless units equations (6)—(10) take the form

$$\frac{d\xi'}{dt'} = -\frac{a_\xi}{b_\eta} \xi' \ln \frac{b_\xi \xi_0 \xi'}{a_\xi} - \frac{c_\xi^{\text{CTL}} \eta_0}{b_\eta} (2 - e^{-\alpha'}) \xi' \eta' - \frac{d_\eta^{\text{chemo}}}{b_\eta} (2 - e^{-\zeta'}) (1 - e^{-\varphi}) \xi', \quad (11)$$

$$\frac{d\eta'}{dt'} = \frac{V_\eta}{b_\eta \eta_0} + \frac{a_\eta \zeta_0}{b_\eta} \eta' \zeta' - \eta' - \frac{d_\eta^{\text{chemo}}}{b_\eta} (2 - e^{-\zeta'}) (1 - e^{-\varphi}) \eta', \quad (12)$$

$$\frac{d\zeta'}{dt'} = \frac{V_\zeta(t)}{b_\eta \zeta_0} + \frac{a_\zeta}{b_\eta \zeta_0} \frac{\xi'}{\xi' + K'_\xi} - \frac{\tilde{a}_\eta \eta_0}{b_\eta} \eta' \zeta' - \frac{c_\zeta \xi_0}{b_\eta} \xi' \zeta', \quad (13)$$

$$\frac{d\varphi}{dt'} = \frac{V_\varphi(t)}{b_\eta} - \frac{b_\varphi}{b_\eta} \varphi \quad (14)$$

$$\frac{d\alpha'}{dt'} = \frac{V_\alpha(t)}{b_\eta \alpha_0} - \frac{b_\alpha}{b_\eta} \alpha'. \quad (15)$$

Then, dropping prime notation for convenience, one finally obtains the following scaled model

$$\dot{\xi} = -h_1 \xi \ln \frac{h_2 \xi}{h_1} - h_3 (2 - e^{-\alpha}) \xi \eta - c_1 (2 - e^{-\zeta}) (1 - e^{-\varphi}) \xi, \quad (16)$$

$$\dot{\eta} = h_4 + h_5 \eta \zeta - \eta - c_2 (2 - e^{-\zeta}) (1 - e^{-\varphi}) \eta, \quad (17)$$

$$\dot{\zeta} = i(t) + \frac{h_6 \xi}{\xi + K'_\xi} - h_7 \eta \zeta - h_8 \xi \zeta, \quad (18)$$

$$\dot{\phi} = a(t) - b\phi, \quad (19)$$

$$\dot{\alpha} = ia(t) - ia_2\alpha, \quad (20)$$

where $h_1 = a_\xi/b_\eta$, $h_2 = b_\xi\xi_0/b_\eta$, $h_3 = c_\xi^{\text{CTL}}\eta_0/b_\eta$, $c_1 = d_\xi^{\text{chemo}}/b_\eta$, $h_4 = V_\eta/b_\eta\eta_0$, $h_5 = a_\eta\xi_0/b_\eta$, $c_2 = d_\eta^{\text{chemo}}/b_\eta$, $i(t) = V_\zeta(t)/b_\eta\xi_0$, $h_6 = a_\zeta/b_\eta\xi_0$, $K'_\xi = K_\xi/\xi_0$, $h_7 = \tilde{a}_\eta\eta_0/b_\eta$, $h_8 = c_\zeta\xi_0/b_\eta$, $a(t) = V_\phi(t)/b_\eta$, $b = b_\phi/b_\eta$, $ia(t) = V_\alpha(t)/b_\eta\alpha_0$, and $ia_2 = b_\alpha/b_\eta$.

3 Steady state analysis

Before proceeding any further, let us perform a steady state analysis of the system (16)—(20). To this end, we will consider the system

$$\dot{\xi} = -h_1\xi \ln \frac{h_2\xi}{h_1} - h_3\xi\eta, \quad (21)$$

$$\dot{\eta} = h_4 + h_5\xi\eta - \eta, \quad (22)$$

$$\dot{\zeta} = \frac{h_6\xi}{\xi + K'_\xi} - h_7\eta\xi - h_8\xi\zeta, \quad (23)$$

which follows from (16)—(20) at $V_i(t) = 0$ ($i = \zeta, \phi, \alpha$) and $\phi(0) = \alpha(0) = 0$.

A possible way to perform the steady state analysis is to use isoclines. Let us consider the phase plane $\xi\eta$, which shows the interactions between two main cell populations: tumor cells and CTL. In this case, the equations for horizontal and vertical isoclines are written as

$$(h_4 - \eta)(\xi + K'_\xi)(h_7\eta + h_8\xi) + h_5h_6\xi\eta = 0, \quad (24)$$

$$\eta = -\frac{h_1}{h_3} \ln \frac{h_2\xi}{h_1}, \quad \xi = 0. \quad (25)$$

The fixed points are situated at the intersections of isoclines (24) and (25). Our analysis shows that the system (21)—(23) has the unstable point $(0, h_4, 0)$ at any choice of parameters. This point lies at the intersection of isoclines (24) and $\xi = 0$.

It is suggested that one of the possible reasons why tumors cannot be recognized and eliminated by the immune system is insufficient antigen presentation on the surface of tumor cell [27]. If the tumor cells do not possess antigens of MHC-II, an activation of helper T cells will depend on the processing of tumor antigens by APC. As previously noted, the more AG-MHC-II complexes will be expressed on APC, the more is the probability of helper T cell activation by APC. Therefore, it is appropriate to consider a_ζ (characterizing the antigen presentation) as a varying parameter and analyse the model outcomes for different values of a_ζ .

A bifurcation diagram for the dimensionless parameter h_6 is presented in Fig. 1. As is seen, there are two bifurcation points. Therefore one can distinguish three main dynamical regimes. For a low antigen presentation ($h_6 < h_{6min}$) the system (21)—(23) has two fixed points: a saddle point $(0, h_4, 0)$ and an improper node (ξ_3, η_3, ζ_3) . This means that under a deficiency in the production of IL-2, the

population of tumor cells is able to escape from the immune response. The tumor grows and the immune system becomes suppressed. In the region $h_{6min} < h_6 < h_{6max}$ there appear two additional fixed points: a stable spiral (ξ_1, η_1, ζ_1) and an unstable saddle (ξ_2, η_2, ζ_2) . Therefore different regimes can exist depending on the initial conditions. First, when initial CTL population size is sufficiently large to reduce a tumor population, the regression of tumor up to a small fixed size takes place where the dynamical equilibrium between tumor and immune system is reached. In this case, the tumor manifests itself via the excited immune system. Second regime appears when initial number of CTL is not large enough to drive the system at the dynamical equilibrium point (ξ_1, η_1, ζ_1) , which is stable spiral. Thus, the tumor grows to a highest possible size, which is defined for the tumor population being in conditions of restricted feeding. The dynamical equilibrium between the tumor and the immune system is reached at the fixed point (ξ_3, η_3, ζ_3) that is an improper node. Finally, for high antigen presentation ($h_6 > h_{6max}$) the fixed points (ξ_2, η_2, ζ_2) and (ξ_3, η_3, ζ_3) disappear. As a result, there are two fixed points: a saddle point $(0, h_4, 0)$ and a stable spiral (ξ_1, η_1, ζ_1) . In this case, a decrease in tumor size is found when the equilibrium between the tumor and the immune system is established.

4 Numerical experiments

Let us briefly discuss now the results presented by de Pillis et al. (2006) in [11]. They consider therapeutic effects using two parameter sets: mouse parameters and human parameters (for two patients), which have been estimated on the basis of experimental data. Their model has either two or four fixed points depending on parameter values which include a tumor-free, two finite-tumor and a high-tumor equilibrium points. The tumor-free fixed point is unstable as long as one of the model parameters (cytolytic potential of NK cells) is smaller than its first bifurcation point. The unstable finite-tumor equilibrium points disappear as this parameter is increased. When the parameter surpasses second bifurcation point, the system has only two fixed points: the stable tumor-free and the stable high-tumor point. Thus the progression of the disease is found to depend on the initial tumor size.

For parameters given in [11] the tumor-free equilibrium point is unstable. Therefore taken alone, the immune system is not able to fight a growing tumor. It was concluded that “any treatment must not only reduce tumor burden, but it must also change the parameters of the system itself. The role of immunotherapy, therefore might be interpreted in this context as a treatment which changes system parameters by, for example, permanently raising the cytolytic potential of the natural killer cells”.

The conclusions made in [11] are the following. First, the high efficiency of combination therapy for mice was shown. The combination therapy includes chemotherapy and immune cells (TIL treatments) given simultaneously. In this case, full regression of the tumor is observed in contrast to effects of chemotherapy and immunotherapy taken separately. Separate treatments stimulate the deceleration of tumor growth, that is, the tumor achieves its maximum size a few days later than in the absence of treatment. Second, numerical calculations with the human data show that a possibility of full tumor regression caused by chemotherapy depends on chemotherapy dosing regimen. There were considered two regimens: chemotherapy pulses administered either once every 5 days or once every 10 days. For the first regimen the tumor is found to die by day 50 while in

the second case it regrows. The full tumor regression is possible for immunotherapy based on TIL injection followed by short doses of IL-2. The existence of this regime depends on the initial tumor size. The regimen of combination therapy considered in [11] results in full tumor regression. Considering vaccine therapy as parametric perturbation of the model [11] shows that the full tumor regression is possible only in the case of combination vaccine therapy with certain regimen of chemotherapy. Finally, as was shown in [11], efficiency of different treatment regimens depends on many factors: sort of tumor, its initial size, a condition of the immune system as well as on chemotherapy dosing regimen.

Let us consider the behavior of our model under chemotherapy and immunotherapy, as well as combined therapy using parameter set in Table 1. Notice that we use the parameter set for (P.1) in the next five subsections. Some preliminary remarks are in order. First, the chosen treatment regimens differ from [11]. Second, the immunotherapy is suggested to base on the use of either IL-2 alone or its combination with IFN- α . Third, we consider the case of low-immunogenic tumor, when antigen presentation is not sufficiently high to stimulate a strong immune response. For this reason, regardless of the tumor size at the termination of course of treatment (the regime I in Fig. 1) our model predicts that the tumor will inevitably regrow. Notice that the initial size of tumor cell population is taken to be large enough to be detectable. As indicated above, the proposed model can be applied for the description of early stages of tumor growth. Finally, at the stage II of malignant melanoma both chemotherapy and immunotherapy are usually administered after surgical treatment. Therefore, in our consideration the initial tumor size is assumed to take a hypothetical value of $\xi(0) \sim 8 \times 10^6$ cells.

4.1. Chemotherapy

Let us test the behavior of our model under a treatment approach which employs nine pulsed doses of chemotherapy, each dose represented by setting $V_\phi(t) = 1$ in (9) for a day, and given once every 5 days (Fig. 2d). As is seen from Fig.2a, for low-immunogenic tumor regression is not observed and the tumor population grows. Number of tumor cells oscillates in time as a result of pulsed character of dosing. Notice that tumor growth rate is found to decrease in comparison with the case without treatment. This is completely due to chemotherapeutic influence because the CTL dynamics is slightly affected by chemotherapy (see Fig. 2b). A possible reason is that an increase in CTL proliferation caused by increasing IL-2 concentration is compensated by death of CTL under the action of chemo-drug. Thus, our study shows that chemotherapy results in stunted tumor growth. In particular, at our choice of parameters the tumor achieves its dangerous size about ten days later than in the absence of the therapy.

4.2. Immunotherapy

IL-2 alone

Let us consider the effect of the therapy with IL-2 alone. For this purpose, the following regimen of the therapy is supposed: four pulsed doses of IL-2, each is equal to 10 MU/day for four days, and administered every 10 days. As is seen from Fig. 2a, this therapy results in a tumor remission with the duration of about

40 days. Notice that in the case of low-immunogenic tumors the regime of full tumor regression is not allowed. As IL-2 concentration grows, the CTL population is also increased approximately by a factor of 7 in 40 days (see Fig. 2b). CTL kill tumor cells and during the therapy course the tumor regression takes place. However, approximately ten days after treatment cessation the IL-2 concentration decreases (see Fig. 2c). At the same time, the CTL population also regresses and, as a result, the tumor growth revives. Thus, this course of treatment leads to a temporary remission only (for 1—1.5 months in our case).

IL-2 plus IFN- α

Let us consider a combined course of the immunotherapy, when IL-2 and IFN- α are given simultaneously. The dose administration pattern for IL-2 is considered to be the same as in the previous subsection. Together with IL-2 the IFN- α at the dose 5 MU/day for four days in a 10 day cycle is administered (Fig. 2d). As is shown in Fig. 2a, there is a substantial decrease in the number of the tumor cells during the cure. At the same time, the tumor remission becomes more pronounced in comparison with the previous case although the regression time is almost the same.

Thus, our study shows that immunotherapy is more effective in the remission time of the tumor as compared with chemotherapy. As another conclusion, the IL-2 alone therapy should be considered as more sparing treatment in comparison with the case of IL-2+IFN- α . Indeed, in spite of better tumor remission for IL-2+IFN- α treatment the IL-2 alone therapy is less toxic.

4.3. Sequential chemo/immunotherapy

In three next subsections, we study the effects of chemotherapy followed immediately by immunotherapy or vice versa as well as the concurrent biochemotherapy. As is known, trials of possible sequential schedules for treatment of metastatic melanoma are conducted at MDACC (see e.g. [4]). Unfortunately, the sequential regimens suggested at MDACC cannot be used in our analysis. As stated above, the model (6)—(10) describes only the early stages of cancer when angiogenesis, invasion and metastases are not taken into account. On the contrary, one of the major tasks accomplished at MDACC is killing the metastases. In particular, they advance the complexes of chemotherapeutic drugs rather than any single-agent chemotherapy.

We consider the following sequential therapy regimen: one pulse of chemotherapy is presented by setting in (9) $V_\varphi(t) = 1$ per day for four days (Fig. 3d). During next four days one pulse of IL-2 therapy is administered in amounts of $V_\zeta(t) = 10$ MU/day in (7). Fig. 3a shows the obtained dynamics of tumor cells. As is seen, the regimen of the suggested sequential therapy does not lead to the tumor regression. However, a markedly stunted tumor growth is observed (tumor cell population reaches the maximum value about thirty days later in this case). At the initial stage ($t < 8$ days), the tumor growth deceleration is entirely due to chemotherapeutic impact. Furthermore, the tumor cell population slightly decreases. This effect is caused by an increase of the IL-2 concentration during eight days (see Fig. 3c), which leads to both a recovery of the CTL number (that has been decreased by chemotherapy) and its following increase (see Fig. 3b). Later on, the tumor steadily grows and the suppression of the immune functions takes place. Notice, that tumor growth rate at this stage is smaller than for $t < 8$

days. Thus, although this sequential regimen does not lead to the tumor regression it allows one to delay the tumor growth.

4.4. Sequential immuno/chemotherapy

Let us consider the following sequential regimen: one pulse of the IL-2 therapy, which is presented by setting in (8) $V_{\zeta}(t) = 10$ MU/day for four days. Next four days one pulse of chemotherapy is administered in dose $V_{\phi}(t) = 1$ in (9) per day for four days (Fig. 3d). The dynamics of tumor cells is shown in Fig. 3a. As is seen, the result of this sequential regimen is worse in comparison with the previous case. Indeed, the IL-2 dosing leads to the increase of its concentration (Fig. 3c) and, accordingly, to the increase of the CTL number (Fig. 3b). However, the CTL have not enough time to achieve the magnitude sufficient for realization of the immune reaction since their growth is abruptly stopped due to chemotherapy (see Fig. 3b). Nevertheless, at the termination of course of treatment the CTL number again increases due to a sufficiently high concentration of IL-2. As a result, the tumor growth becomes slower reaching a dangerous size twenty days later than in the absence of therapy.

4.5. The concurrent biochemotherapy

Let us consider the following regimen of the sequential therapy: the chemotherapy in dose $V_{\phi}(t) = 1$ per day and the IL-2 therapy in dose $V_{\zeta}(t) = 7$ MU/day are given simultaneously for four days. First of all, let us note that the concurrent biochemotherapy is found to be less toxic in comparison with other sequential regimens (see, e.g., [5]). To take proper account of this fact, the dose of the IL-2 is selected to be approximately $3 \cdot 10^6$ units less than in subsections 4.3 and 4.4. As a result, the tumor cell dynamics becomes a little higher in comparison with the first sequential regimen in 4.3 during a long enough period of time except for the initial interval of (0; 10) days (see Fig. 3a). For this period of time, the tumor growth deceleration is more pronounced in comparison with the case of chemo/immuno sequence. Indeed, since chemotherapy and IL-2 therapy are used simultaneously, the tumor cells die under the action of both drug and the immune response recovered by IL-2 therapy. As is seen from Fig. 3b, the dynamics of CTL is similar to that without therapy. Notice that for the first six days the IL-2 concentration is higher than in the case of chemo/immunotherapy (Fig. 3c). Thus, simulations performed within our model show that the stronger increase of the IL-2 population prevents the reduction in the CTL number caused by the chemical impact (unlike the first sequential regimen). In turn, for the next four days the IL-2 concentration becomes lower as compared with the case of chemo/immunotherapy. Therefore, one can conclude that the concurrent biochemotherapy is more favorable in comparison with the regimen considered in the subsection 4.3.

4.6. Vaccine therapy

Cancer vaccines are considered as one of promising methods of immunotherapy. Using vaccine allows sensitizing the immune system to the presence of the certain forms of cancer. As a consequence, the immune system will be able to find and lyse tumor cells more effectively. When vaccine appears in the body the anti-tumor lymphocyte formation occurs. The efficacy of the vaccination depends on the following factors:

1. The number of tumor cells and their mitotic activity;

2. The sort of tumor, i.e. its histological structure, antigen structure, the number of HLA-A molecules expressed on the tumor cells;
3. Initial conditions of the immune system.

There are a few known different kinds of cancer vaccines that consist of either living tumor cells or some tumor-derived proteins, peptides and gangliosides [30]. For instance, some vaccines include HLA-A1, A2, A3 and HLA-DR restricted tumor peptides. Clinical trials of this vaccine for treatment of malignant melanoma [32,33] show that the vaccination leads to the development of peptide-specific immune responses in 75—80% of patients and is associated with clinical tumor regressions in a proportion of patients. Notice that both GM-CSF and IL-2 were used in these experiments as an adjuvant. The observed toxicity of this vaccination is probably due to low doses of IL-2. There were also revealed atypical skin reactions in one or two patients, which were not caused by IL-2.

In this subsection, we consider a cancer vaccine consisting of four tumor-derived peptides with an adjuvant (see [38]). As long as antigen/adjuvant complexes may stimulate immune response to vaccine thereby enhancing immune reaction to patient's tumor cells, effect of the vaccination can be taken into account through the model parameters. Therefore, in order to simulate vaccine therapy we change the values of four model parameters at the time of vaccination (in a similar manner as in [11]). The sensitive to vaccination parameters can be extracted from the experimental results obtained on mouse vaccine trials by Diefenbach et al. (2001) [12]. Namely, we fitted the experimental curves produced by Diefenbach's data to our model and found the parameters that would change to reflect the administration of a therapeutic vaccine. They are c_{ξ}^{CTL} , the rate of inactivation of tumor cells by CTL, a_{η} , the rate of CTL proliferation induced by IL-2, a_{ζ} , the antigen presentation (the probability of interaction between helper T cell precursors and APC), and \tilde{a}_{η} , the rate of consumption IL-2 by CTL. Finally, to simulate vaccine therapy we alter the corresponding model parameters in the same direction as they change in Diefenbach's murine model [12] (cf. [11]). As a result, all four parameters (c_{ξ}^{CTL} , a_{η} , a_{ζ} , and \tilde{a}_{η}) are found to be increased.

The regimen of vaccination chosen for simulation of vaccine therapy is the following: the cancer vaccine administered once a week during 1—3, 5—7, 13, 27, 40, and 53 weeks, respectively [38]. It should be noted that we will present here the results for vaccine therapy alone, so that we put $V_{\varphi}(t)$, $V_{\zeta}(t)$, $V_{\alpha}(t)$ equal to zero as well as $\alpha = \varphi = 0$ in (6)-(10). In fact, we have studied within our model the regimen of combined vaccine and chemotherapy as well. For this simulation the chemotherapeutic drug dose was taken in accordance with the experimental regimen considered in [38]. However, our study shows that the regimen of combined vaccine and chemotherapy gives the results very similar to the case of vaccine therapy alone.

Before we proceed further, let us discuss briefly an important issue concerning an individual immunologic and clinical outcome from using the same vaccine for different patients. To this end, we consider the experimental results found by Slingluff in [32]. For instance, for several patients the T cell response to the vaccine was found to be not strong enough to decrease the tumor size and, as a result, the tumor was progressing. At the same time, the tumor regression was observed for two other patients with immune responses to one or more peptides used in the vaccine. Thus, CTL response by itself does not guarantee the tumor

regression. This fact may be explained by heterogeneity of the tumor antigen expression. In order to reflect a possibility of different responses to vaccination we will conditionally divide patients in two groups and suggest some characteristic parameter sets for each group (see Table 1). We assume that in both cases tumor has the same histological structure (for instance, melanoma) with equal doubling time and carrying capacity (actually, these characteristics may vary between tumor specimens). Additionally, the lifetime of cytotoxic T lymphocytes is chosen to be the same. On the other hand, the tumor antigen expression (c_{ξ}^{CTL}), the strength of the immune response (a_{ζ} , a_{η} , \tilde{a}_{η} and c_{ζ}), and the reaction to vaccination are taken to be specific for each group (see (26) and (27) below). As before, we consider low-immunogenic tumors. In this case, the progressive tumor growth is observed at any initial conditions of the immune system (see Fig. 4, solid lines), i.e. the first steady state condition takes place (see Fig. 1, region I).

Let us consider the case of the first group of patients (with the parameter set P.1 in Table 1). From the above discussion it is clear that the values of parameters c_{ξ}^{CTL} , a_{η} , a_{ζ} , and \tilde{a}_{η} will depend on the regimen of vaccination, i.e. on time. We choose the following dependence:

$$c_{\xi}^{\text{CTL}} = \begin{cases} 5.28 \times 10^{-9}, & t \in (5; 448), \\ 4.4 \times 10^{-9}, & t < 5 \text{ and } t > 448, \end{cases} \quad a_{\eta} = \begin{cases} 11.4 \times 10^{-9}, & t \in (3; 448), \\ 9.9 \times 10^{-9}, & t < 3 \text{ and } t > 448, \end{cases} \quad (26)$$

$$a_{\zeta} = \begin{cases} 1.92 \times 10^7, & t \in (3; 448), \\ 1.6 \times 10^7, & t < 3 \text{ and } t > 448, \end{cases} \quad \tilde{a}_{\eta} = \begin{cases} 4.29 \times 10^{-9}, & t \in (3; 448), \\ 3.3 \times 10^{-9}, & t < 3 \text{ and } t > 448, \end{cases}$$

where t is measured in days.

Under these assumptions, the steady-state conditions become changed in such a way that the system (21)—(23) passes to the region II on the bifurcation diagram (see Fig.1 and Fig. 4). In this region, treatment outcome depends already on the initial tumor size and the immune system conditions. Fig. 5 shows the results for two courses of the vaccination: the first one was administered without delay while the second one was administered 10 days later, when tumor cell population has reached a sufficiently large value to escape the immune response (Fig. 5a, 5b, 5c).

Let us analyze first the case of a small initial tumor size when it takes the hypothetical value of $\xi(0) = 8 \times 10^6$ cells. This is a quite reasonable estimation when the course of vaccine therapy is used after previous surgery. For therapy without delay, this number of tumor cells is enough to induce the immune response. As is seen from Fig.5c, the IL-2 concentration grows and, consequently, the CTL number is increased. The integral curves tend to the stable spiral point and the long tumor remission is observed (Fig. 5a). As is seen from (26), 83 days after the last injection the system parameters are restored to their initial values. As a result, the system returns into the region I of the bifurcation diagram and the tumor growth is recommenced. Therefore, the revaccination is required.

Assumed 10-day delay is simulated by a time displacement $t \rightarrow t + 10$ in (26). In this case, the tumor had time to reach a sufficiently large size and both the IL-2 concentration and CTL number were decreasing (Fig. 5b and c). The integral curves tend to the improper node, which means progressive tumor. The

simulations show that the earlier the vaccination is administered the more effective it is for the cancer treatment. Notice that the considered duration of the vaccine action (exactly 83 days) is not imperative. It seems plausible that this action may last even longer. Anyway, the revaccination is required after that to avoid a disease recurrence.

In order to simulate the vaccine administered without any previous treatment we assume the tumor size to take a value $\xi(0) = 3 \times 10^7$. Fig. 6a shows that even for therapy without delay the tumor regression does not occur and only some stunted tumor growth with lower saturation level is observed in comparison with the case without therapy. One can suppose that the saturation level without therapy corresponds to a dangerous tumor size in stage II of malignant process. Then the lower saturation level with vaccination may be considered as a steady state of a patient during the vaccine action (Fig. 6a). In the case of 10-day delay, the tumor size almost reaches the therapeutic saturation level (Fig 6a). As is seen, the vaccine-mediated enhancement of the immune response prevents tumor growth to a dangerous size. Namely, after 15 days of growth the tumor curve goes slightly down and tends to the therapeutic saturation level. This does not mean, however, that a delay in the vaccination is not dangerous. In fact, the presented model is valid for the description of the tumor-immune dynamics at early stages (I,II) of tumor. As mentioned above, we do not take into account the angiogenesis, which begins at certain size of the tumor and provokes its further growth [3,7]. In other words, the existence of the saturation level does not imply the termination of the tumor growth. Figs. 6b and 6c show dynamics of CTL and IL-2, respectively. As is seen, the vaccination leads to the increase of the IL-2 concentration and, consequently, to the increase of the CTL number.

Let us consider now the behavior of the second group of patients in response to the vaccination. This group is characterized by a lower antigen expression (c_ξ^{CTL}) and associated with it the weaker immune response (a_ζ , a_η , \tilde{a}_η , and c_ζ) (see Table 1, P.2). We assume the following dependence of model parameters:

$$c_\xi^{\text{CTL}} = \begin{cases} 3.63 \times 10^{-9}, & t \in (5; 448), \\ 3.3 \times 10^{-9}, & t < 5 \text{ and } t > 448, \end{cases} \quad a_\eta = \begin{cases} 11.5 \times 10^{-9}, & t \in (3; 448), \\ 9.6 \times 10^{-9}, & t < 3 \text{ and } t > 448, \end{cases} \quad (27)$$

$$a_\zeta = \begin{cases} 1.82 \times 10^7, & t \in (3; 448), \\ 1.4 \times 10^7, & t < 3 \text{ and } t > 448, \end{cases} \quad \tilde{a}_\eta = \begin{cases} 4.35 \times 10^{-9}, & t \in (3; 448), \\ 2.9 \times 10^{-9}, & t < 3 \text{ and } t > 448, \end{cases}$$

where t is measured in days. As is seen from Fig. 4, in this case the steady-state conditions do not change. This result looks rather unexpected. In fact, it means absence of the positive clinical response despite the fact that the immune reaction to the tumor is taken to be enhanced by the vaccine even better as compared with the first group. Indeed, we have intentionally taken the bigger relative growth of parameters a_η , a_ζ , and \tilde{a}_η in (27) in comparison with (26).

Fig. 7 shows the results of the vaccination after surgery and Fig. 8 shows the case without preliminary treatment. In the first case, using vaccine without delay allows stunting tumor growth and it reaches the therapeutic saturation level in 70 days. Besides, with vaccine the saturation level becomes lower than without therapy. It should be noted that the vaccine administered with 10-days delay is not effective because no deceleration of the tumor growth is observed (Fig. 7a).

Notice also that a reduction of the therapeutic saturation level does not imply the termination of tumor growth. The vaccination is ineffective when it is administered without preliminary surgery (Fig. 8a). Summarizing presented results, one can conclude that efficacy of the vaccination depends on sort of tumor, initial tumor size, and conditions of immune system.

4.7. Comparison with the second group of patients

In subsections 4.1—4.5 we have simulated chemotherapy, immunotherapy, and combination of these treatments using parameter set for the first patient group (Table 1, P.1). At the same time, the results obtained in previous subsection for vaccine therapy show some important differences in behavior of two groups of patients. Therefore, it is interesting to compare the results of chemotherapy, immunotherapy, and combination of these treatments for two groups of patients. To this end, we have simulated the same as in 4.1—4.5 therapeutic regimens for the second group of patients. Our study shows that IL-2 alone therapy does not result in the tumor remission in the second group (see Fig. 9a). Furthermore, tumor size reaches the dangerous value during the same time as for chemotherapy. Thus, both chemotherapy and immunotherapy allow slowing down tumor growth by approximately 10 days more as compared with the case without therapy. However, IL-2 alone therapy leads to more pronounced decrease in tumor growth rate in comparison with chemotherapy. As is seen from Fig. 9a, for IFN- α administered together with IL-2 the tumor growth deceleration becomes more evident than in the case of IL-2 alone therapy. At the same time, it is well known that similarly to IL-2 IFN- α therapy may cause constitutional, hematologic, gastrointestinal, cardiovascular, neurologic and other side effects [5]. Thus, we can conclude that IL-2 alone should be considered as a more favorable treatment in comparison with chemotherapy and IL-2+ IFN- α therapy for the second group as well.

Simulations of sequential treatment regimens using the parameter set (P.2) give the similar to (P.1) results. The only difference is that tumor cell dynamics for (P.2) is found to be similar for chemo/immuno, immuno/chemo as well as concurrent chemo/immunotherapy after termination of treatment. More pronounced tumor growth could be associated with lesser effect of IL-2 therapy for the second group of patients. Indeed, as a result of lower tumor antigen expression, stimulation of CTL proliferation by IL-2 becomes insufficient for effective recognition of the tumor cells. Let us compare effects of both IL-2 alone and vaccine for the second group. As is seen from Figs. 7 and 9, the vaccine therapy is more effective if administered without delay. Besides, Figs. 7c and 9c show that using the vaccine is more sparing therapy in comparison with IL-2 alone therapy. Thus, our study shows that vaccine therapy is the most effective treatment for both groups of patients.

5. Conclusion

We have studied the effects of different treatment regimens on both the tumor growth and the immune response within the mathematical model describing tumor-immune dynamics with chemotherapy and immunotherapy taken into account. The bifurcation diagram shows three main dynamical regimes. For a low antigen presentation the tumor is able to escape from the immune response. For high antigen presentation the decrease of the tumor size is found when the equilibrium between the tumor and the immune system is established. In the case

of the medium antigen presentation there exist two regimens of disease depending on both the initial tumor size and the condition of immune system: (i) the regression to small tumor when the dynamical equilibrium is established and (ii) a progressive tumor growth to the highest possible size in the conditions of limited nutrition.

In order to describe a possibility of different responses to treatment regimens, patients were conditionally divided in two generalized groups. Each group is characterized by specific tumor antigen expression, the strength of the immune response, and the reaction to vaccination. For the first group we found that chemotherapy may result in a deceleration of the tumor growth approximately by 10 days in comparison with the case without therapy. In the case of IL-2 alone therapy, a tumor remission is observed for the whole course of treatment. However, the tumor growth revives after the termination of course of treatment due to a decrease of the IL-2 concentration. Thus, this treatment leads to a temporary tumor remission (for 1—1.5 months in our case). When IFN α is administered together with IL-2 the tumor remission becomes more pronounced in comparison with the previous case although the remission time is found to be almost the same. Therefore, as long as IFN α may cause various side effects, one can conclude that the considered variant of IL-2 alone therapy is more effective for the remission of the tumor as compared with chemotherapy. For the second group the tumor remission was not observed. Nevertheless, our results show that the immunotherapy regimen for the second group is also more effective than chemotherapy.

The simulation of sequential treatment regimens including chemotherapy and IL-2 therapy for the first group shows that chemotherapy followed immediately by IL-2 therapy is the most effective sequence as compared with other considered sequential schedules. In the case of chemotherapy followed immediately by IL-2 therapy, deceleration of the tumor growth is observed. The tumor reaches the dangerous size thirty days later than without therapy. It should be noted that unlike the immuno/chemotherapy sequence, the results of the concurrent biochemotherapy and sequential chemo/immunotherapy are almost coincident (being yet slightly worse for concurrent biochemotherapy). On the other hand, the concurrent regimen is accompanied by a smaller dose of IL-2. For this reason, the concurrent biochemotherapy is less toxic (notice that this fact was also mentioned in [5]) and therefore, is more sparing in comparison with considered chemo/immuno sequence.

Besides, we have simulated vaccine therapy for both groups of patients in two cases: after surgical intervention and without previous treatment. Our study shows that vaccine therapy is more effective than other described treatments when used without time delay from a prescribed date of vaccination after surgery. This means that using vaccine will give the best results for patients with both the small size of tumor and the immune system which is not suppressed by tumor growth and able to response to the vaccine. Thus, our model shows a promising effect of the vaccine treatment to improve immune response to certain forms of cancer, which qualitatively agrees with clinically observed results (see, e.g., [28,32,33,36]).

References

1. Adam, J.A. and Bellomo, N. A survey of Models for Tumor-Immune System Dynamics. Birkhäuser, Boston, MA (1996)
2. Alberts, B., Bray, D., Lewis, J., Raff, M., Roberts, K., Watson, J. D. Molecular biology of the cell (3rd edition). Garland Publishing Inc., New York, 1408pp (1994)
3. Arciero, J.C., Kirschner, D.E., Jackson, T.L.: A mathematical model of tumor-immune evasion and siRNA treatment. *Disc. Cont. Dyn. Syst.-B.* 4. 39—58 (2004)
4. Buzaid A.C.: Strategies for combining chemotherapy and biotherapy in melanoma. *Cancer Control.* 7(2). 185—197 (2000)
5. Buzaid A.C. and Atkins M.: Practical guidelines for the management of biochemotherapy-related toxicity in melanoma. *Clin. Cancer Res.* 7. 2611—2619 (2001)
6. Chao, D. L., Davenport, M. P., Forrest, S., and Perelson, A.S.: A stochastic model of cytotoxic T cell responses. *Journal of Theoretical Biology.* 228. 227—240 (2004)
7. Chaplain, M.A.J.: Mathematical models in cancer research. in *The Cancer Handbook.* Nature publishing group. Chapter 60. 937—951 (2003)
8. De Boer, R.J., Hogeweg, P., Dullens, F.J., De Weger, R.A., Den Otter, W.: Macrophage T lymphocyte interactions in the anti-tumor immune response: a mathematical model. *J. Immunol.* 134. 2748—2758 (1985)
9. De Boer, R.J., Oprera, M., Antia, R., Murali-Krishna, K., Ahmed, R., and Perelson, A. S.: Recruitment times, proliferation, and apoptosis rates during the CD8+ T cell Response to lymphocytic choriomeningitis virus. *Journal of Virology.* 75. 10663—10669 (2001)
10. de Pillis L.G. and Radunskaya A.E.: The dynamics of an optimally controlled tumor model; a case study. *Math. Comput. Model.* 37. 1221—1244 (2003)
11. de Pillis L.G., Gu. W., Radunskaya A.E.: Mixed immunotherapy and chemotherapy of tumors: modeling, applications and biological interpretations. *J. of Theoretical Biology.* 238(4). 841-862 (2006)
12. Diefenbach, A., Jensen, E.R., Jamieson, A.M., Raulet, D.: Rae1 and H60 ligands of the NKG2D receptor stimulate tumor immunity. *Nature.* 413, 165—171 (2001)
13. Farrar, J.D., Katz, K.H., Windsor, J., Thrush, G., Scheuermann, R.H., Uhr, J.W., Street, N.E.: Cancer dormancy. VII. A regulatory role for CD8+ T cells and IFN-gamma in establishing and maintaining the tumor-dormant state. *J. Immunol.* 162(5), 2842—2849 (1999)
14. Garay, R., Lefever, R.: A kinetic approach to the immunology of cancer: stationary states properties of effector-target cell reactions. *J. Theor. Biol.* 73. 417—438 (1978)
15. Garbelli S., Mantovani S., Palermo B., and Giachino C.: Melanocyte-specific, cytotoxic T cell responses in vitiligo: the effective variant of melanoma immunity. *Pigment Cell Res.* 18. 234—242 (2005)
16. Gardner S.N.: A mechanistic, predictive model of dose-response curves for cell cycle phase-specific and nonspecific drugs. *Cancer Res.* 60. 1417—1425 (2000)
17. Gause, B.L., Sznol, M., Kopp, W.C., Janik, J.E., Smith II, J.W., Steis, R.G., Urba, W.J., Sharfman, W., Fenton, R.G., Creekmore, S.P., Holmlund, J., Conlon, K.C., VanderMolen, L.A. and Longo, D.L.: Phase I study of subcutaneously administered interleukin-2 in combination with interferon alfa-2a in patients with advanced cancer. *J. of Clin. Oncol.* 14. 2234—2241 (1996)
18. Hara, I., Hotta, H., Sato, N., Eto, H., Arakava, S. and Kamidono, S.: Rejection of mouse renal cell carcinoma elicited by local secretion of interleukin-2. *J. Cancer Res.* 87. 724—729 (1996)
19. Hu Z., Sun Y., and Alan G.: Targeting tumor vasculature endothelial cells and tumor cells for immunotherapy of human melanoma in a mouse xenograft model. *Proc. Natl. Acad. USA,* 96.. 8161—8166 (1999)
20. Issaeva O.G. and Osipov V.A. Modeling of anti-tumor immune response: immunocorrective effect of centimeter electromagnetic waves. *q-bio: CB/0506006.* (2005)
21. Kirschner, D., Panetta, J. C.: Modeling immunotherapy of the tumor-immune interaction. *J. of Mathematical Biology.* 37. 235—252 (1998)
22. Li J., Guo K., Koh, V.W., Tang J.P., Gan B.Q., Shi H., Li H.X., Zeng Q.: Generation of PRL-3- and PRL-1-specific monoclonal antibodies as potential diagnostic markers for cancer metastases. *Clin. Cancer Res.* 11(6). 2195—2204 (2005)
23. Liu, Y., Ng, Y., and Lillehei, K. O.: Cell mediated immunotherapy: a new approach to the treatment of malignant glioma. *Cancer Control.* 10. 138—147 (2003)
24. Loo, T.J. et al.: Mechanism of action and pharmacology studies with DTIC (NSC-45388) *Cancer Treatment Reports.* 60. 149-152 (1976)

25. O'Byrne, K.J., Dalglish, A.G., Browning, M.J., Steward, W.P., Harris, A.L.: The relationship between angiogenesis and the immune response in carcinogenesis and the progression of malignant disease. *Eur.J.Cancer* 36, 151-169 (2000)
26. Qu Z., Griffiths G.L., Wegener W.A., Chang C.H., Govindan S.V., Horak I.D., Hansen H.J., Goldenberg D.M.: Development of humanized antibodies as cancer therapeutics. *Methods*. 36(1). 84—95 (2005)
27. Roitt, I., Brostoff, J., Male, D.: *Immunology* (6th edition). Mosby, London, 480pp, (2001)
28. Rosenbaum, E., Rosenbaum, I.: *Everyone's guide to cancer supportive care: a comprehensive handbook for patients and their families*. Andrews McMeel Publishing (2005)
29. Rosenberg, S. A. and Lotze, M. T.: Cancer immunotherapy using interleukin-2 and interleukin-2-activated lymphocytes. *Annual Review of Immunology*. 4. 681—709 (1986)
30. Schirmacher, V., Umansky, V., Linder, M., Müerköster, S., Rocha M.: Models for immunotherapy and Cancer Vaccines. in *The Cancer Handbook*. Nature publishing group. Chapter 68. 1055—1068 (2003)
31. Sherrat, J., Nowak, M.: Oncogenes, anti-oncogenes and the immune response to cancer: a mathematical model. *Proc. R. Soc. London B V*. 248. 261—271 (1992)
32. Slingluff Jr C.L., Petroni G.R., Yamshchikov G.V., Barnd D.L., Eastham S., Galavotti H., Patterson J.W., Deacon D.H., Hibbitts S, Teates D., Neese P.Y., Grosh W.W., Chianese-Bullock K.A., Woodson E.M.H., Wiernasz C.J., Merrill P, Gibson J., Ross M., Engelhard V.H.: Clinical and immunologic results of randomised phase II trial of vaccination using four melanoma peptides either administered in GM-CSF in adjuvant or pulsed on dendritic cells. *J. Clin. Oncol.* 21(21). 4016—4026 (2003)
33. Slingluff Jr C.L., Petroni G.R., Yamshchikov G.V., Hibbitts S., Grosh W.W., Chianese-Bullock K.A., Bissonette E.A., Barnd D.L., Deacon D.H., Patterson J.W., Parekh J., Neese P.Y., Woodson E.M.H., Wiernasz C.J., and Merrill P.: Immunologic and clinical outcomes of vaccination with a multiepitope melanoma peptide vaccine plus low-dose interleukine-2 administered either concurrently or on a delayed schedule. *J. Clin. Oncol.* 22(22). 4474—4485 (2004)
34. Stepanova, N.: Course of the immune reaction during the development of a malignant tumor. *Biophysics*. 24, 917—923 (1980)
35. Sznol M. and Davis T.: Antibodies and recombinant cytokines. in *The Cancer Handbook*. Nature publishing group. Chapter 87, 1371—1379 (2003)
36. Wheeler C.J., Asha D., Genatao L., Yu J.S., Black K.L.: Clinical responsiveness of glioblastoma multiforme to chemotherapy after vaccination. *Clin. Cancer Res.* 10. 5316—5326 (2005)
37. www.emedicine.ru
38. <http://www.nci.nih.gov/clinicaltrials>

Figure captions

Fig. 1. A bifurcation diagram varying the antigen presentation (h_6). For $h_6 < h_{6min}$ there is only one steady state — improper node (region I). When $h_{6min} < h_6 < h_{6max}$ there are two stable steady states — improper node and spiral node as well as an unstable (saddle) point (region II). For $h_6 > h_{6max}$ only one steady state, the spiral node remains (region III).

Fig. 2. Human data. Group (P.1, see Table 1). Effects of chemo-, IL-2 and IL-2 plus IFN- α therapies on tumor and immune response dynamics. (a) tumor cells, (b) cytotoxic T cells, and (c) IL-2 vs. time. (d) shows drug administration pattern: nine doses, strength $V_\phi(t) = 1$, 1 day per dose on a 5 day cycle, and IFN- α administration pattern: four doses, strength $V_\alpha(t) = 5$ MU/day, 4 days per dose on a 10 day cycle. IL-2 is administered with four doses of strength $V_\zeta(t) = 10$ MU/day, 4 days per dose on a 10 day cycle. Initial conditions: 8×10^6 tumor cells, 2.25×10^7 cytotoxic T lymphocytes, 2.4×10^7 IL-2 units. The case without therapy is shown by solid lines.

Fig. 3. Human data. Group (P.1, see Table 1). Effects of one pulse of chemotherapy followed immediately by one pulse of IL-2-therapy, one pulse of IL-2 therapy followed immediately by one pulse of chemotherapy, and concurrent biochemotherapy. (a) tumor cells, (b) cytotoxic T cells, and (c) IL-2 vs. time. (d) shows drug administration pattern: one pulsed dose of chemotherapy, strength $V_\phi(t) = 1$ per day, 4 days per dose for sequential chemo/immunotherapy (dotted line), sequential immuno/chemotherapy (dash-dot line), and concurrent biochemotherapy (gray line). IL-2 administration pattern: one pulsed dose of strength $V_\zeta(t) = 10$ MU/day, 4 days per dose after chemotherapy (chemo/immunotherapy sequence) or before chemotherapy (immuno/chemotherapy sequence) and $V_\zeta(t) = 7$ MU/day for four days simultaneously with chemotherapy (concurrent biochemotherapy). Initial conditions: 8×10^6 tumor cells, 2.25×10^7 cytotoxic T lymphocytes, 2.4×10^7 IL-2 units. The case without therapy is shown by solid lines.

Fig. 4. Bifurcation diagrams showing the effect of vaccine therapy on anti-tumor immune response dynamics for both groups of patients.

Fig. 5. Human data. Group (P.1, see Table 1). Effects of vaccine administered after surgery without delay and with delay for 10 days. (a) tumor cells, (b) cytotoxic T cells, and (c) IL-2 vs. time. Initial conditions: 8×10^6 tumor cells, 2.25×10^7 cytotoxic T lymphocytes, 2.4×10^7 IL-2 units. The case without vaccine is shown by solid lines.

Fig. 6. Human data. Group (P.1, see Table 1). Effects of vaccine administered without previous treatment and with delay for next 10 days. (a) tumor cells, (b) cytotoxic T cells, and (c) IL-2 vs. time. Initial conditions: 3×10^7 tumor cells, 1.35×10^7 cytotoxic T lymphocytes, 1.8×10^7 IL-2 units. The case without vaccine is shown by solid lines.

Fig. 7. Human data. Group (P.2, see Table 1). Effects of vaccine administered after surgery without delay and with delay for 10 days. (a) tumor cells, (b) cytotoxic T cells, and (c) IL-2 vs. time. Initial conditions: 8×10^6 tumor cells, 2.25×10^7 cytotoxic T lymphocytes, 2.4×10^7 IL-2 units. The case without vaccine is shown by solid lines.

Fig. 8. Human data. Group (P.2, see Table 1). Effects of vaccine administered without previous treatment and with delay for next 10 days. (a) tumor cells, (b) cytotoxic T cells, and (c) IL-2 vs. time. Initial conditions: 3×10^7 tumor cells, 1.35×10^7 cytotoxic T lymphocytes, 1.8×10^7 IL-2 units. The case without vaccine is shown by solid lines.

Fig. 9. Human data. Group (P.2, see Table 1). Effects of chemo-, IL-2 and IL-2 plus IFN- α therapies on tumor and immune response dynamics. (a) tumor cells, (b) cytotoxic T cells, and (c) IL-2 vs. time. Treatment regimens are chosen to be the same as in Fig. 2d. Initial conditions: 8×10^6 tumor cells, 2.25×10^7 cytotoxic T lymphocytes, 2.4×10^7 IL-2 units. The case without therapy is shown by solid lines.

Table 1. Estimated values of the parameters.

| Parameter | Units | Description | Estimated value | Source |
|-------------------------|--------------------------------------|--|--|-------------------------|
| a_ξ | day ⁻¹ | Tumor growth rate | 0.13 | [19] |
| b_ξ | cell ⁻¹ day ⁻¹ | a_ξ/b_ξ is tumor carrying capacity | 3×10^{-10} | [19] |
| c_ξ^{CTL} | cell ⁻¹ day ⁻¹ | Rate of tumor cells inactivation by CTL | 4.4×10^{-9} (P.1) 3.3×10^{-9} (P.2) | |
| V_η | cell day ⁻¹ | Rate of steady inflow of CTL | $7,3 \times 10^6$ | [15] |
| a_η | cell ⁻¹ day ⁻¹ | CTL proliferation rate induced by IL-2 | 9.9×10^{-9} (P.1) 9.6×10^{-9} (P.2) | |
| b_η | day ⁻¹ | CTL death rate | 0.33 | [6] |
| a_ζ | unit day ⁻¹ | Antigen presentation | 1.6×10^7 (P.1) 1.4×10^7 (P.2) | |
| \tilde{a}_η | cell ⁻¹ day ⁻¹ | Rate of consumption of IL-2 by CTL | 3.3×10^{-9} (P.1) 2.9×10^{-9} (P.2) | |
| c_ζ | cell ⁻¹ day ⁻¹ | Inactivation of IL-2 molecules by prostglandines | 1.8×10^{-8} (P.1) 1.5×10^{-8} (P.2) | |
| K_ξ | cell | Half-saturation constant | 3×10^6 | |
| d_ξ^{chemo} | day ⁻¹ | Tumor cell killing by chemotherapy | 0.9 | [11] |
| d_η^{chemo} | day ⁻¹ | CTL killing by chemotherapy | 0.6 | [11] |
| b_ϕ | day ⁻¹ | Decay rate of chemotherapy drug | 6.4 | [24] |
| b_α | day ⁻¹ | Decay rate of therapeutic IFN- α | 1.7 | [37] |
| $\xi_0 = 10^8$ cells | | $\eta_0 = 9 \times 10^7$ cells | $\zeta_0 = 2 \times 10^7$ units | $\alpha_0 = 10^7$ units |

P.1 and P.2 mean the first and the second groups of patients, respectively.

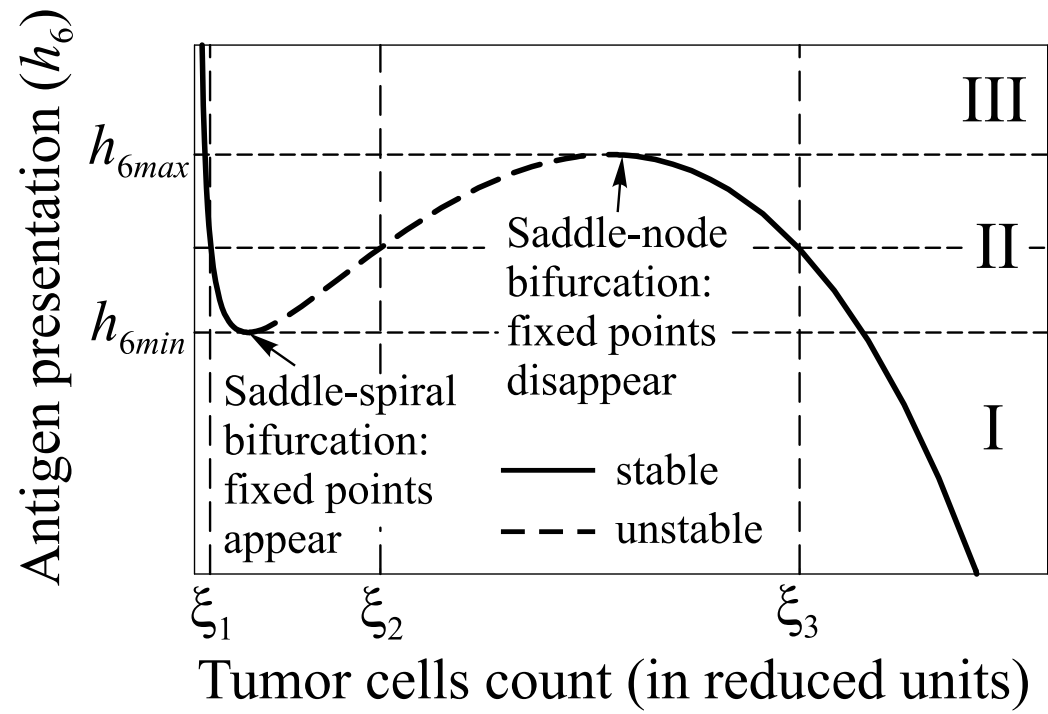
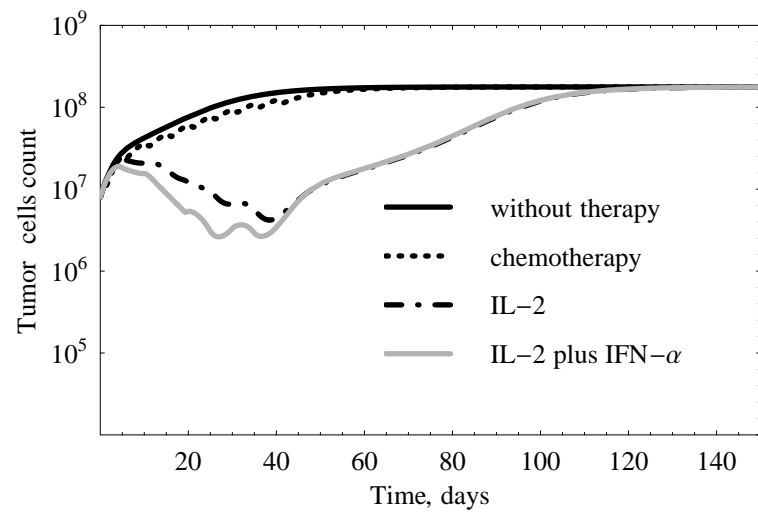
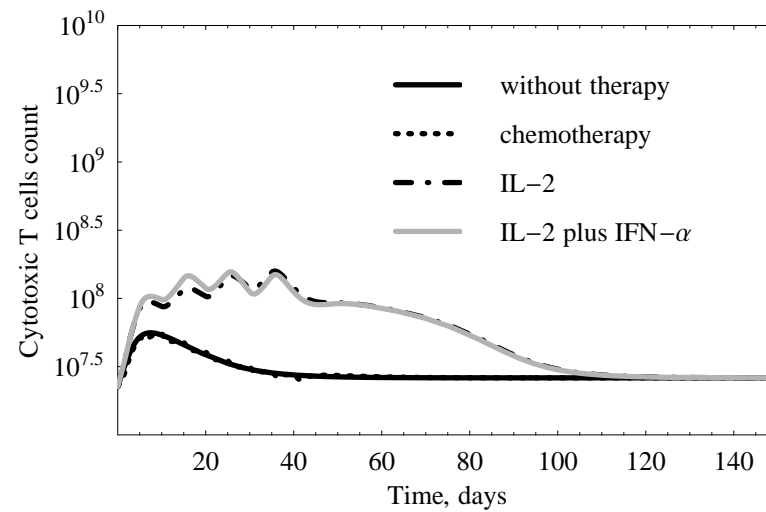


Fig.1

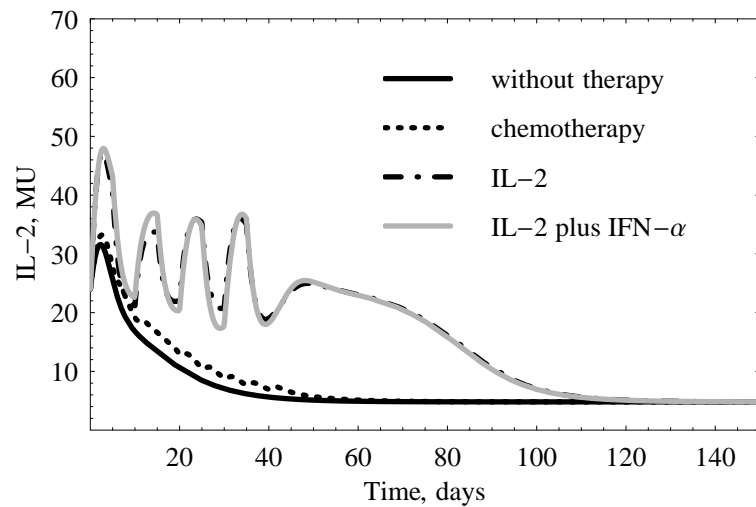
a



b



c



d

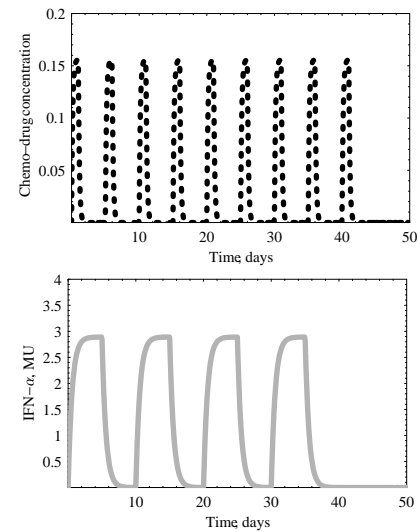
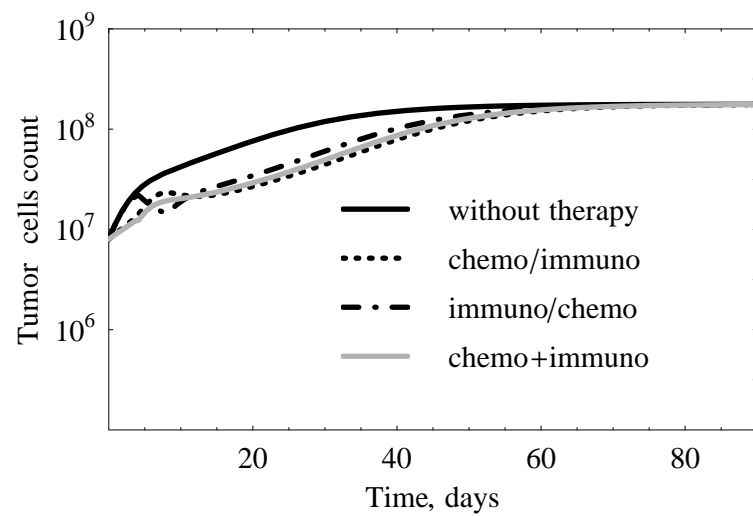
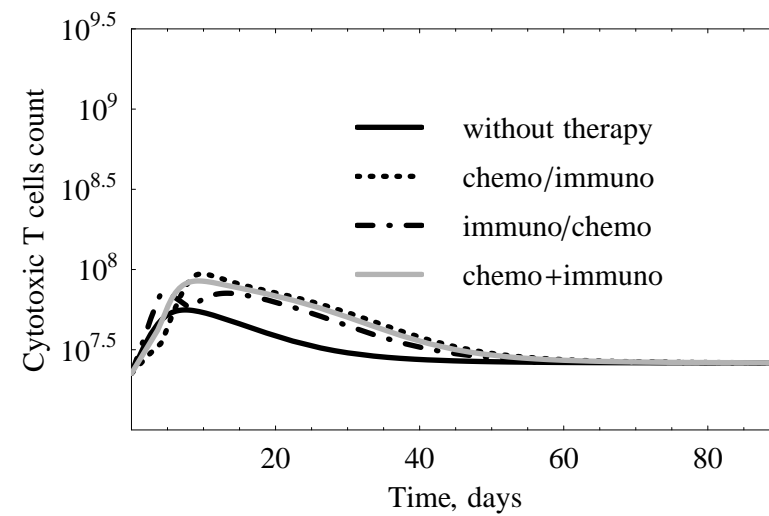


Fig. 2

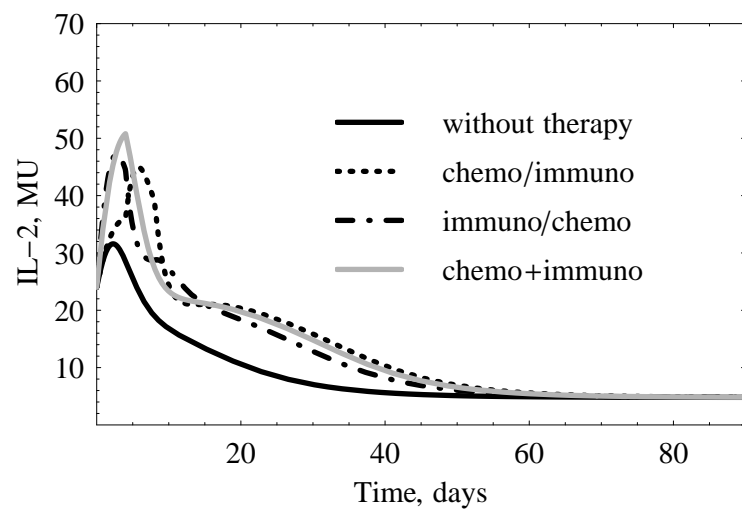
a



b



c



d

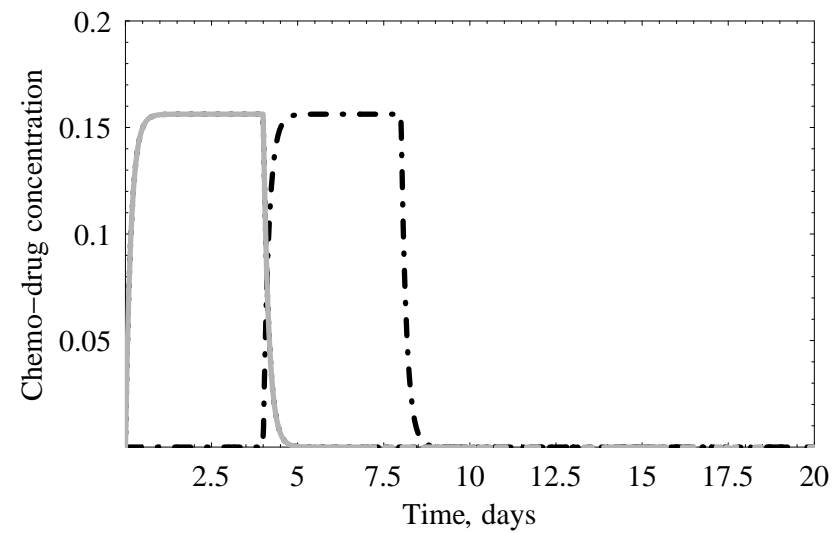


Fig. 3

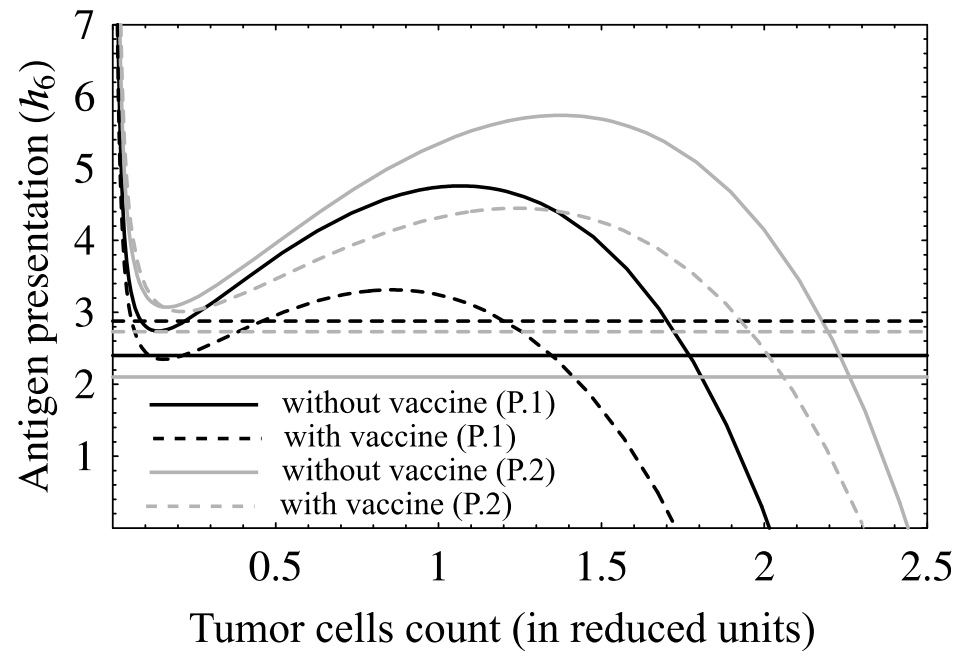


Fig. 4

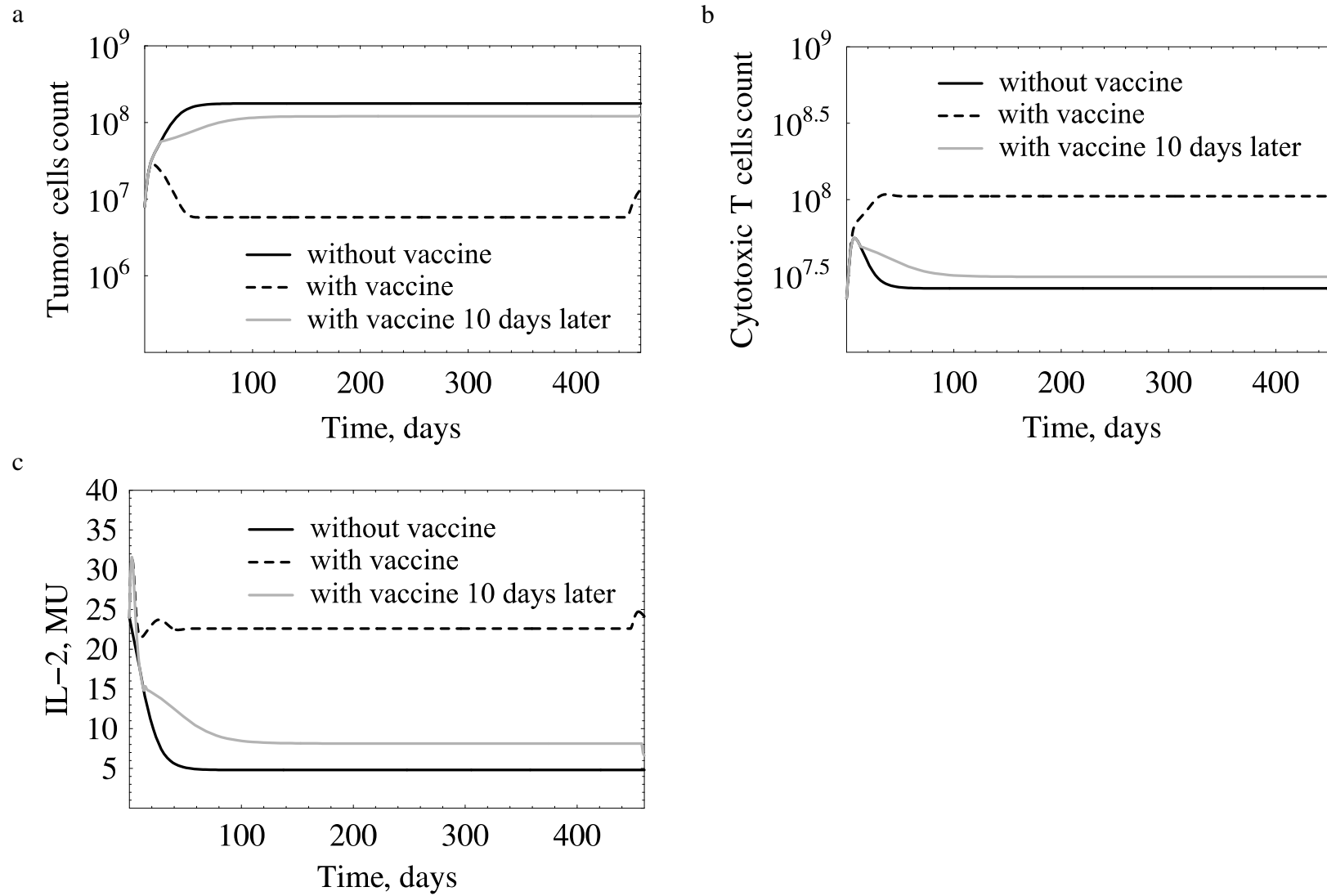


Fig. 5

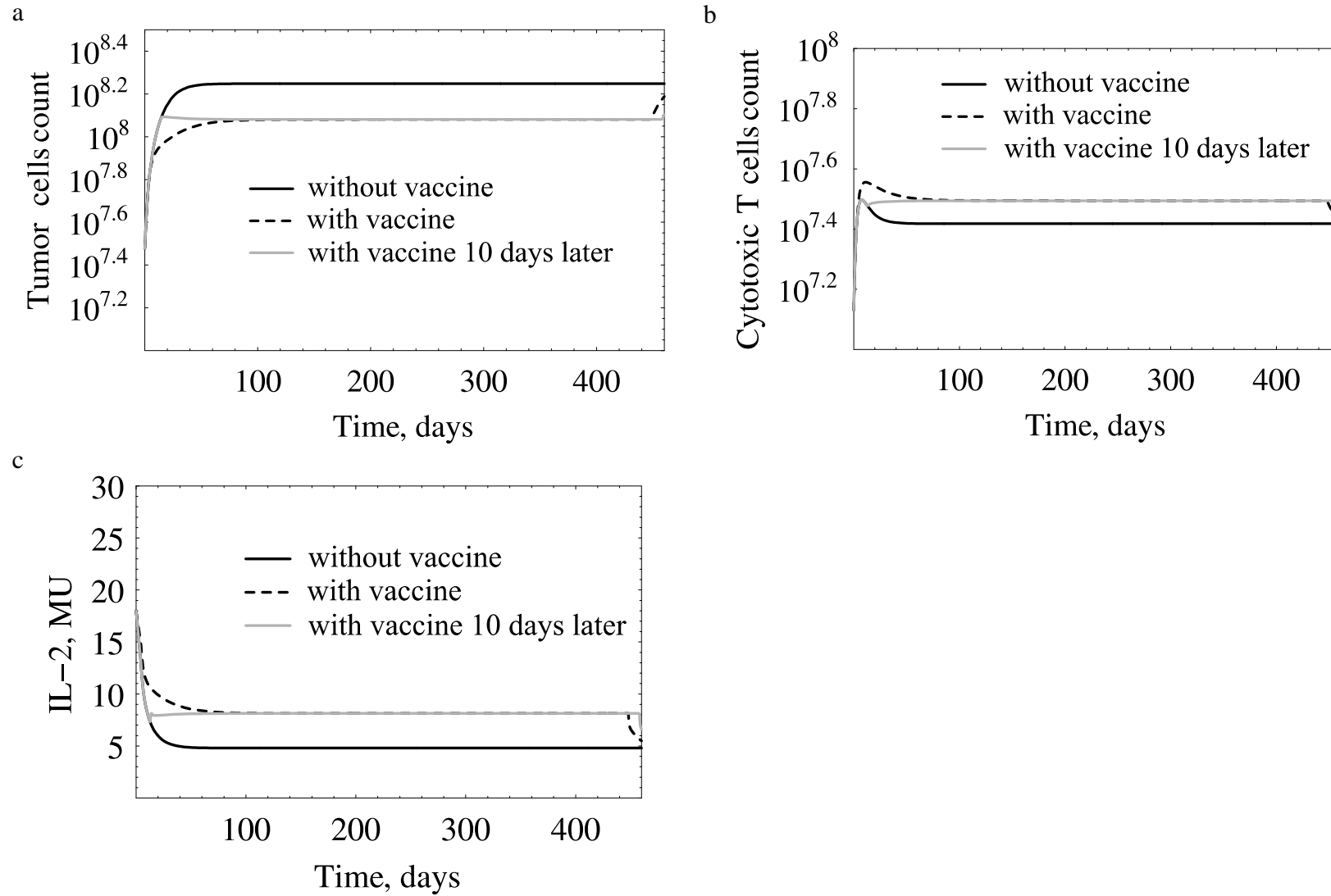


Fig. 6

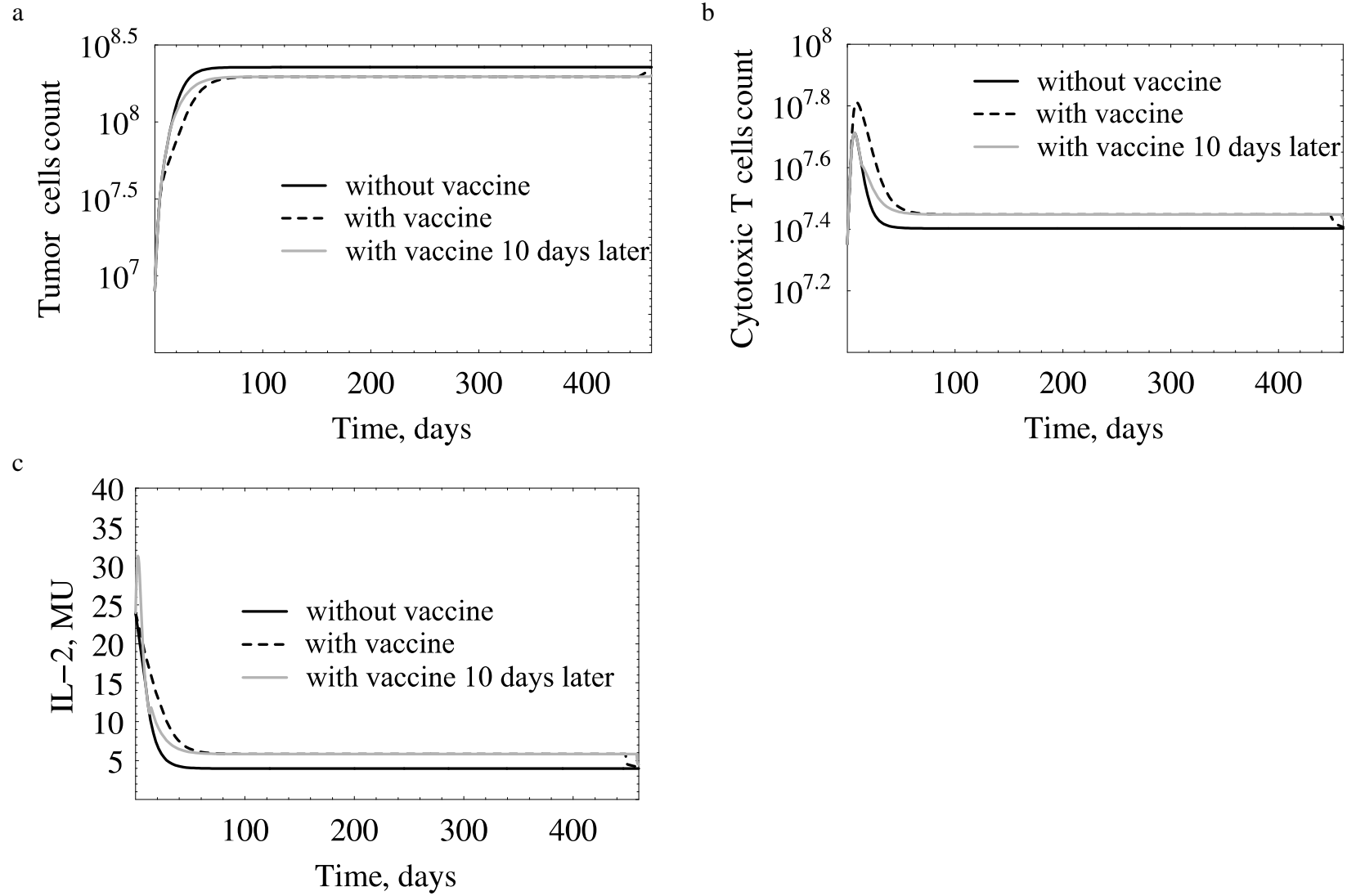


Fig. 7

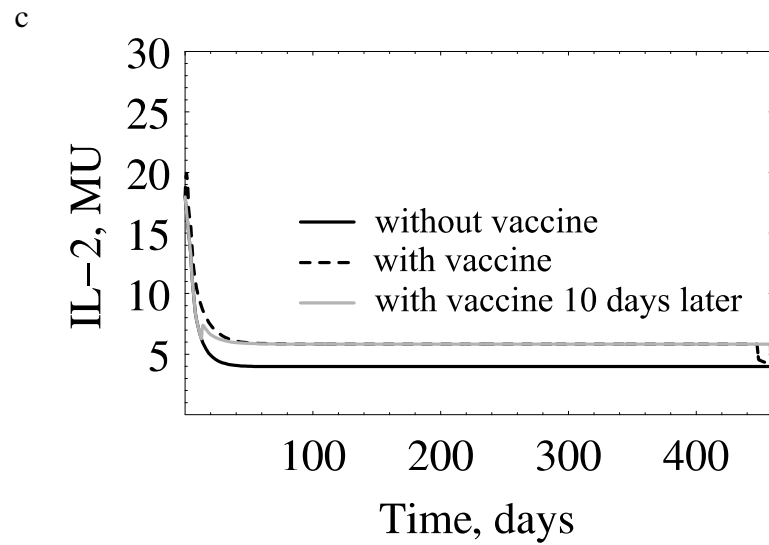
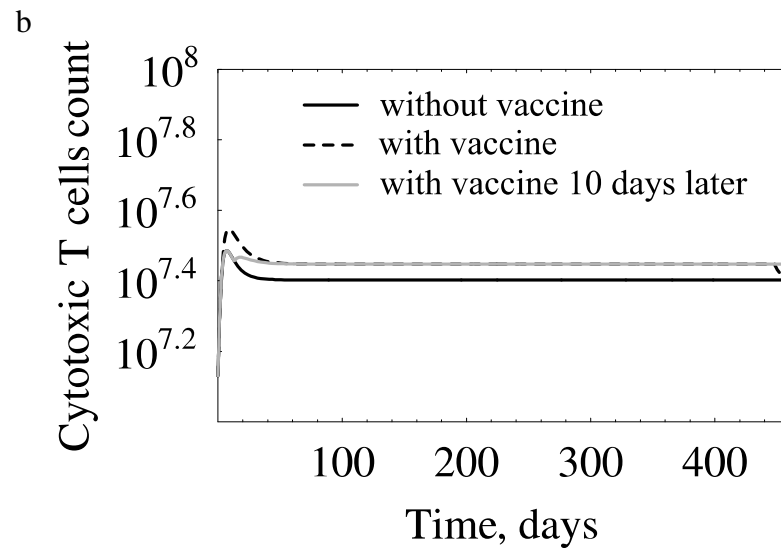
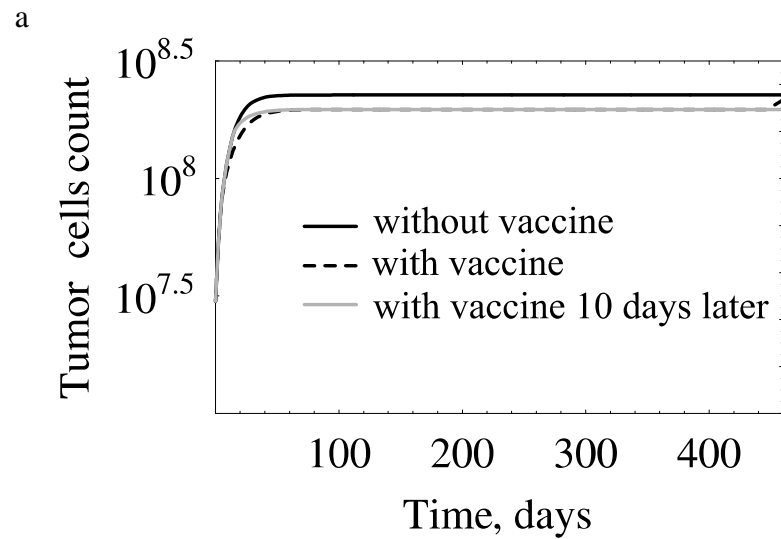
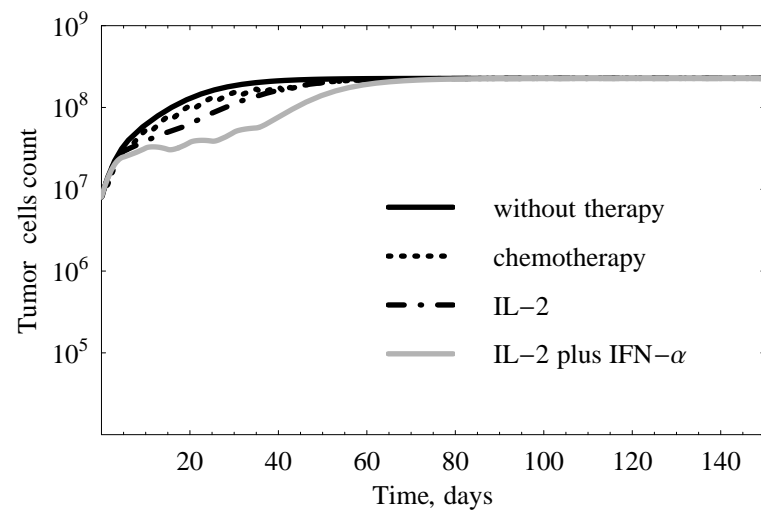
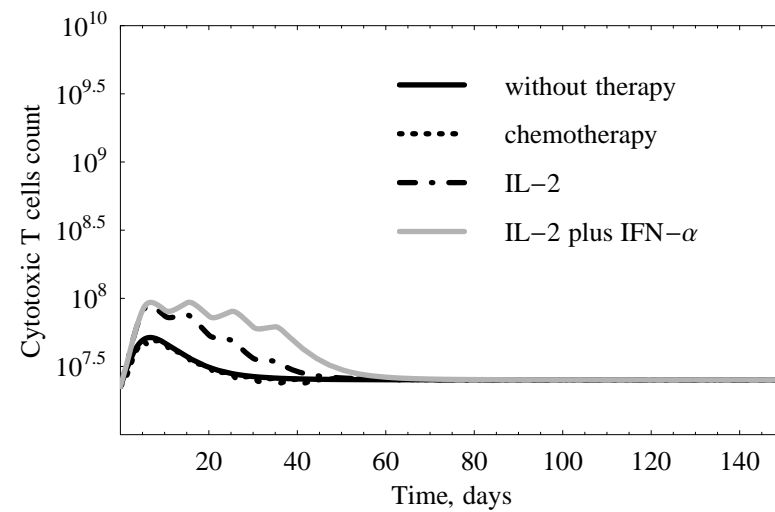


Fig. 8

a



b



c

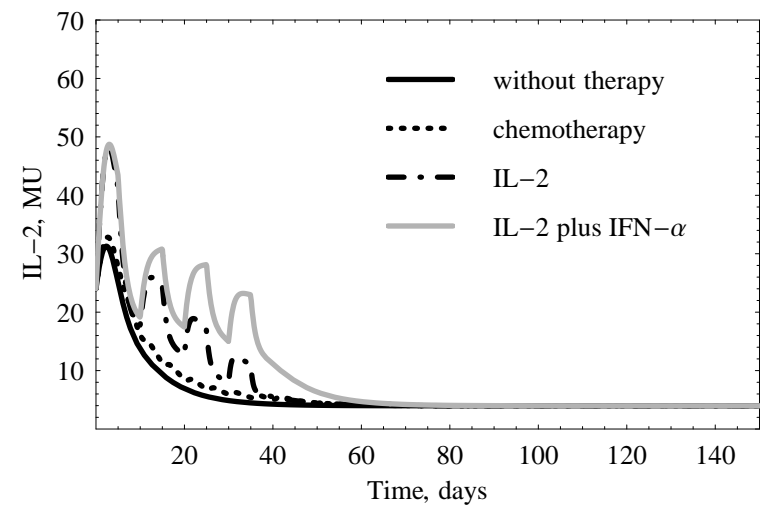


Fig. 9